

Development of a Chaff Dispense Program for Target Tracking Radar Deception

Min-Joon Choi¹, Je-Hong Park², Min-Seok Jie², Won-Hyuk Choi^{2,*}

¹Avionics Software Development Center, Republic of Korea Air Force, Seosan-Si, Korea

²Department of Avionics Engineering, Hanseo University, Seosan-Si, Korea

Received 10 November 2022; received in revised form 27 January 2023; accepted 14 February 2023

DOI: <https://doi.org/10.46604/peti.2023.11150>

Abstract

This study aims to develop an appropriate chaff dispensing program to deceive the target tracking radar (TTR) effectively. Chaff is a countermeasure commonly used by fighter aircraft to deceive TTR. However, there has been a lack of methodology for calculating chaff dispense programs that take into account the specific characteristics of the fighter, chaff, and TTR. This study proposes a methodology that considers these variables to calculate chaff dispense programs and addresses this gap. The proposed method is demonstrated through TESS engagement, which shows its effectiveness in various engagement situations.

Keywords: chaff, TTR, chaff dispense program, electronic warfare, TESS

1. Introduction

Chaff is a popular passive countermeasure that enables fighter aircraft to against target tracking radar (TTR) [1]. It is composed of a bundle of conductive wires that creates a larger radar cross section (RCS) than the RCS of a fighter, misleading the TTR into tracking the chaff cloud instead of a fighter as a target [2]. To deceive the TTR, some chaff must be burst to create an RCS larger than the fighter's RCS before the fighter passes through a radar resolution cell (RRC) of the TTR [3]. Several articles have been published on effective chaff dispense program calculation.

For example, Žák et al. [4] present an appropriate interval for bursting chaff to deceive radar in certain example situations. However, the lack of specification of the correlations among the variables used to calculate the interval makes it challenging to apply this method to other engagement situations.

Wu et al. [5] present a model for calculating the chaff dispense program based on missile approach time, airplane movement, and chaff cloud movement. Nevertheless, this model does not consider variables such as the RCS of airplanes and chaff, or the variables used in the TTR to calculate RRC. Shengliang et al. [6] use the characteristics of the chaff cloud and radar to calculate the chaff dispense program, but this method relies on ship-based calculations and may not be suitable for fighter engagement situations.

As a result, there is currently no methodology for calculating the chaff dispense program that takes into account the characteristics of the fighter, chaff, TTR, and engagement situation. This study presents a methodology for calculating the chaff dispense program that considers variables such as the fighter and engagement situation. In addition, this study analyzes the deceptive effect of the calculated chaff dispense program against the TTR through engagement simulations.

* Corresponding author. E-mail address: choiwh@hanseo.ac.kr

2. Methodology for Chaff Dispense Program

The following assumptions are required for the calculation of a chaff dispense program. When a fighter dispenses chaff while passing through an RRC, the first chaff dispensed creates a larger RCS than the later chaff. As a result, it can be concluded that minimizing the interval between bursts or dispensing multiple chaff simultaneously is more effective in creating a larger RCS before the fighter passes through the RRC. However, electromagnetic coupling and shielding of chaff limit the increase in RCS from dispensing chaff at very short intervals or multiple chaff bursts compared to a single chaff cartridge [7-8]. For this study, it is assumed that the chaff RCS remains constant regardless of the chaff dispense sequence. To adjust for the discrepancy between the actual RCS of chaff and the estimated RCS, a coefficient value of 0.5 is applied to the chaff RCS [9].

A chaff dispense program is designed to maximize the effectiveness of chaff in deceiving TTR during engagements. This program takes into account various factors, such as the RCS of the fighter, the RCS of the chaff, the TTR, and the engagement situation.

$$BC = \lceil 2\sigma_a / \sigma_c \rceil \quad (1)$$

The burst count (BC) equation is derived to enhance the efficacy of chaff. It takes into consideration the fighter's RCS (σ_a), the RCS of single chaff (σ_c), and the number of chaffs to be dispensed. Eq. (1) calculates the number of chaffs to be dispensed by rounding up to the nearest integer the result of multiplying the fighter's RCS (σ_a) by the coefficient of 2 and then dividing that value by the RCS of single chaff (σ_c). The coefficient of 2 represents the minimum ratio of chaff RCS to fighter RCS required to deceive TTR [10].

$$\sigma_a = \begin{pmatrix} a_{-180}e_{-90} & a_{-180}e_{-80} & \cdots & a_{-180}e_{80} & a_{-180}e_{90} \\ a_{-170}e_{-90} & a_{-170}e_{-80} & \cdots & a_{-170}e_{80} & a_{-170}e_{90} \\ \vdots & \vdots & \vdots & \vdots & \vdots \\ a_{170}e_{-90} & a_{170}e_{-80} & \cdots & a_{170}e_{80} & a_{170}e_{90} \\ a_{180}e_{-90} & a_{180}e_{-80} & \cdots & a_{180}e_{80} & a_{180}e_{90} \end{pmatrix} \quad (2)$$

The fighter's RCS (σ_a) is represented as a two-dimensional matrix, with azimuth angles (a) ranging from -180 to 180 degrees and elevation angles (e) ranging from -90 to 90 degrees, as shown in Eq. (2). However, when calculating the burst count (BC) using Eq. (1), only the exposed RCS value is necessary. This value is adjusted based on the fighter's yaw angle (Y), pitch angle (P), and slant angle (S) with respect to the TTR.

$$\sigma_a = \sigma_a \left[(180 - Y)/10, (90 - S - P)/10 \right] \quad (3)$$

Eq. (3) represents the formula for the exposed RCS (σ_a) in the two-dimensional matrix as a function of the fighter's yaw angle (Y), pitch angle (P), and slant angle (S) between the TTR and the fighter. Eq. (3) provides information on how the fighter's orientation affects the RCS, covering a range of -180 to 180 degrees for azimuth angles (a) and -90 to 90 degrees for elevation angles (e). Additionally, the equation also takes the adjustments made to the RCS based on the yaw, pitch, and slant angles of the fighter.

$$\sigma_c = 0.5 \times \sigma_{MaxRCS} \times BR(T_c) \quad (4)$$

The RCS of chaff (σ_c) is determined by multiplying the maximum RCS (σ_{MaxRCS}) of chaff for each frequency band by the chaff's bloom rate (BR) over the time (T_c) it takes for the fighter to pass through the RRC, as shown in Eq. (4). To account for the difference in polarization between the chaff and the TTR's antenna, a coefficient factor of 0.5 is applied [9]. This equation considers various factors, such as the maximum RCS of chaff, the chaff's bloom rate, and the time it takes for the fighter to pass through the RRC, to calculate the RCS of chaff.

$$\sigma_{MaxRCS} = 0.17N\lambda^2 \quad (5)$$

The maximum RCS of chaff (σ_{MaxRCS}) can be calculated by multiplying the square of the wavelength, the number of dipoles (N), and the coefficient factor 0.17 [11].

Fig. 1 shows the change in bloom rate (BR) of chaff over time, with the curved graph plotting the percentage of the maximum RCS achieved by chaff against time in seconds since being burst. The graph shows that after 0.5 seconds of being burst, chaff has a bloom rate of 60% compared to its maximum RCS [12].

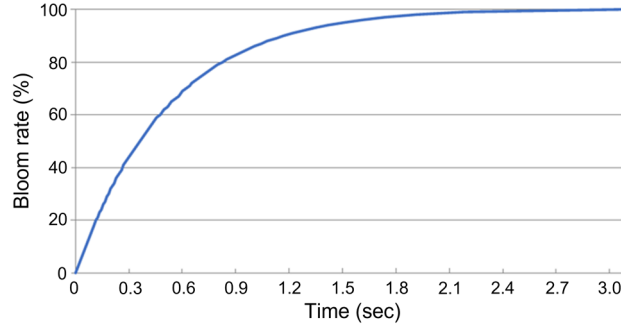


Fig. 1 The bloom rate of chaff

$$T_c = L/V \quad (6)$$

T_c is the time it takes for a fighter to pass through the length (L) of the RRC, calculated by dividing L by the speed (V) of the fighter. The calculation of L depends on whether the angle at which the fighter will pass through RRC (Φ) is greater than or less than the slant angle of RRC (Φ_r), assuming the fighter passes through the central point of the RRC. Fig. 2 shows the RRC, L , Φ , Φ_r , and the fighter passing through RRC depending on the engagement situation.

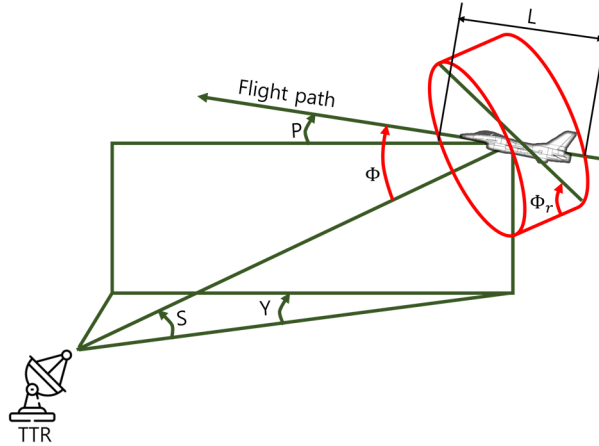


Fig. 2 Engagement situation

$$\Phi = \cos^{-1}(\cos S \cos Y \cos P - \sin S \sin P) \quad (7)$$

$$\Phi_r = \tan^{-1}(E/d) \quad (8)$$

The angle at which a fighter will pass through RRC (Φ) is determined by the slant angle (S) between the TTR and fighter, the yaw angle (Y), and the pitch angle (P). The slant angle of RRC (Φ_r) is determined by the cylindrical section (E) of RRC and the range gate width (d) of the TTR. The range gate width of the TTR (d) is typically 1.2 times the pulse width.

$$E = \frac{SR\theta_{az} \times SR\theta_{el}}{\sqrt{(SR\theta_{el})^2 \cos^2 \theta + (SR\theta_{az})^2 \sin^2 \theta}} \quad (9)$$

Eq. (9) represents the formula for the cylindrical section (E) of RRC, and it includes variables such as the slant range (SR) between the TTR and fighter, the azimuth/elevation beamwidth (θ_{az}, θ_{el}) of TTR's antenna. Other variables used in the equation are calculated based on the pitch angle (P), yaw angle (Y), and slant angle (S) of the fighter [13]. Detailed information about these variables can be found in Table 1.

Table 1 Variables needed for calculating the cylinder section

Variables	Calculating
$\cos^2\theta$	$\frac{(\cos P \sin Y)^2}{(\cos P \sin Y)^2 - (\cos S \sin P + \sin S \cos P \cos Y)^2}$
$\sin^2\theta$	$\frac{(\cos S \sin P + \sin S \cos P \cos Y)^2}{(\cos P \sin Y)^2 - (\cos S \sin P + \sin S \cos P \cos Y)^2}$

To calculate the length (L) of the RRC that a fighter will pass through, two cases are considered by comparing Φ and Φ_r . The first case occurs when a fighter enters the base of the RRC and passes through the opposite base. The second case occurs when a fighter enters the RRC pillar and passes through the opposite pillar.

$$\text{Case 1: } 0^\circ \leq \Phi \leq \Phi_r \text{ or } 180^\circ - \Phi_r \leq \Phi \leq 180^\circ$$

$$L = \frac{c \times d}{2|\cos \Phi|} \tag{10}$$

c is the speed of light.

$$\text{Case 2: } \Phi_r \leq \Phi \leq 180^\circ - \Phi_r$$

$$L = \frac{E}{\sin \Phi} \tag{11}$$

$$BI = T_c / BC \tag{12}$$

The burst interval (BI) is calculated by dividing the time required for the fighter to pass through the RRC (T_c) by the BC .

3. Simulation and Results

In this paper, the deception effectiveness of the chaff dispense program against TTR is confirmed using Leonardo's tactical engagement simulation software (TESS). TESS is a high-resolution modeling software based on MATLAB and Simulink that simulates the engagement situation between a fighter and a weapon system, including TTR [14]. By considering various factors such as the engagement environment, ECM, fighter's maneuverability, and miss distance between the fighter and missile, TESS provides the probability of kill for the fighter [15]. Since TESS does not provide the tracking information during the simulation, the chaff dispensing program's deception effectiveness is evaluated by counting the number of scenarios in which the miss distance between the fighter and the missile is within a range of 25 m [16].

The miss distance of 25 m is twice the blast radius of the warhead carried by the SA-3 missile. Initially, the SA-8 missile's warhead blast radius was considered as the basis for the modeled weapon system in TESS, but it was later decided to use the SA-3's warhead instead due to the SA-8's warhead blast radius of only 5 meters, which was considered too short to produce meaningful results. [17].

The weapon system that engages the fighter is "S-CGN-HA-R", provided as a basic model in TESS. It tracks the target through TTR and guides a missile to the target using command guidance radar. The waveform of TTR in "S-CGN-HA-R" is composed of pulses of electromagnetic waves with a frequency of 6 GHz, transmitted at intervals of 100 μ s and a duration of

1.5 μ s. The beam width of the electromagnetic waves transmitted by the TTR is 3° . The target tracked by TTR is “Fighter”, a basic model provided in TESS. The RCS of “Fighter” is specified in Table 2. Each row and column in Table 2 shows the size of the RCS reflected when tracking the fighter at the exposed angle.

Table 2 Fighter RCS as dBm² for 6Ghz

El Az	-90	-80	-70	-60	-50	-40	-30	-20	-10	0	10	20	30	40	50	60	70	80	90
-180	38.42	34.87	13.27	0.89	6.33	8.66	9.63	7.69	7.08	21.54	9.94	2.55	0.94	-0.4	2.38	4.63	14.14	37.04	40.32
-170	36.11	20.82	2.7	0.8	13.05	10.96	8.91	2.91	0.33	8.03	1.88	-3.21	-6.57	-5.06	-2.39	-2.7	3.52	22.55	37.82
-160	36.14	19.23	0.25	-0.2	12.67	7.32	-1.31	-1.65	-6.04	1.11	-3.36	-4.39	-4.92	-9	-4.9	-3.57	1.33	21.04	37.81
-150	36.28	21.49	-0.08	-2.85	-2.09	-2.52	-4.88	-2.72	-7.85	-3.71	-5.73	-4.79	-4.97	-4.18	-7.11	-3.06	8.07	19.34	38.11
-140	36.4	15.1	5.75	-6.07	-5.88	-4.65	-3.98	-5.24	-7.07	-1.13	-8.24	-9.9	-8.56	-5.68	-5.99	-1.85	8.42	11.85	37.82
-130	36.14	18.26	9.98	0.13	-3.94	-8.2	-3.84	-6.54	-6.51	0.3	-8.35	-8.27	-6.01	-6.13	-6.19	-4.36	9.77	12.58	37.75
-120	36.1	18.83	13.13	13.24	2.09	-3.51	-1.83	-5.74	-5.83	2.36	-3.75	-8.58	-6.9	-5.57	-2.03	5.39	13.74	12.54	37.72
-110	36.14	20.79	19.11	15.31	12.31	6.53	5.8	0.54	1.94	10.89	4.4	0.48	0.62	8.55	10.99	13.39	14.47	13.83	37.7
-100	36.39	26.24	22.35	21.23	18.97	12.34	17.08	11.83	12.96	17.45	10.96	10.05	9.11	14.54	17.48	19.93	18.31	22.42	37.82
-90	36.38	29.44	28.97	24	27.33	28.89	29.22	25.85	25.12	26.45	25.96	26.87	27.35	26.82	27.65	27.69	26.9	24.88	37.9
-80	36.39	23.3	20.87	12.14	14.85	12.22	10.93	8.67	9.68	15.6	14.27	16.39	15.22	12.46	18.31	18.96	16.74	20.76	37.82
-70	36.14	17.09	10.08	11.98	8.34	10.06	9.98	6.45	2.7	6.11	10.63	10.6	7.67	11.56	14.85	11.92	12.49	16.8	37.7
-60	36.1	12.32	4.41	6.37	3.93	4.11	0.76	2.74	4.55	7	4.16	5.22	4.05	4.88	11.77	13.71	6.32	17.08	37.72
-50	36.14	13.61	7.35	2.72	2.76	3.42	-0.7	-1.05	-3.19	0.3	-7.66	0.09	3.19	1.85	4.32	10.03	9.56	18.82	37.75
-40	36.4	25.2	8.2	0.78	1.94	-2.63	-4.57	-4.53	-3.89	-3.37	-6.29	-1.68	-4.18	2.39	4.46	6.93	8.98	22.42	37.82
-30	36.28	21.07	5.13	3.68	2.31	-4.27	-5.21	-8.08	-4.84	-5.92	-6	-9.94	-1.71	1.41	5.22	4.8	10.9	27.71	38.11
-20	36.14	9.37	4.14	3.63	-3.4	-5.99	-3.99	-5.94	-5.1	-4.76	-4.76	-2.84	0.82	6.94	15.58	5.83	9.74	19.35	37.81
-10	36.11	8.51	7.17	5.36	-2.46	-8.02	-6.62	-4.6	-0.95	-2.96	-4.04	-3.77	8.91	11.1	15.85	6.7	13.14	16.89	37.82
0	38.42	17.71	8.59	8.18	1.85	0.25	-3.34	-1.16	2.2	6.38	-0.64	-3.49	9.61	9.84	4.63	9.35	16.5	19.73	40.32
10	36.11	8.4	7.15	5.36	-2.35	-7.57	-6.45	-4.36	-0.76	-3.14	-4.25	-3.97	8.93	11.09	15.86	6.68	13.1	16.9	37.82
20	36.14	9.57	4.11	3.51	-3.46	-5.69	-3.79	-5.83	-5.18	-4.89	-4.83	-2.81	0.78	6.9	15.58	5.77	9.83	19.34	37.81
30	36.28	21.02	5.16	3.72	2.34	-4.31	-5.47	-7.77	-4.62	-6.06	-6.21	-10	-2.17	1.37	5.18	4.84	10.89	27.72	38.11
40	36.4	25.2	8.26	0.79	2.16	-2.69	-5.33	-4.4	-3.63	-4.19	-7.61	-2.1	-4.9	2.17	4.35	6.87	8.92	22.42	37.82
50	36.14	13.7	7.38	2.64	2.61	3.55	-1.32	-0.64	-2.7	-0.52	-9	0.18	3.65	2.07	4.49	10.09	9.57	18.78	37.75
60	36.1	12.41	4.45	6.35	3.88	4.05	0.77	2.97	4.44	6.43	4.27	5.27	4.08	5	11.69	13.66	6.33	17.09	37.72
70	36.14	17.03	9.92	12.06	8.34	10.04	9.95	6.64	1.34	6.14	10.63	10.66	7.71	11.56	14.85	11.86	12.44	16.91	37.7
80	36.39	23.33	20.92	12.37	14.09	12.59	11.04	8.6	9.79	15.78	14.44	16.52	15.35	12.19	18.36	18.96	16.88	20.83	37.82
90	36.38	29.49	28.97	24.09	27.26	28.92	29.45	25.86	25.11	26.46	25.85	26.89	27.32	26.85	27.84	28.01	27.02	24.86	37.9
100	36.39	26.23	22.4	21.3	18.99	12.32	16.98	11.75	12.85	17.46	10.98	9.84	8.93	15.26	17.49	20.05	18.34	22.47	37.82
110	36.14	20.78	19.1	15.3	12.47	6.46	5.58	0.39	2.04	10.69	4.42	0.26	0.91	8.4	10.78	13.45	14.53	13.89	37.7
120	36.1	18.87	13.18	13.28	2.36	-2.66	-2.14	-5.64	-5.29	2.3	-3.59	-8.13	-6.49	-5.78	-2.02	5.34	13.71	12.64	37.72
130	36.14	18.26	9.99	0.1	-3.34	-7.97	-4.51	-6.12	-7.44	0.18	-8.66	-8.29	-5.86	-6.38	-6.46	-4.27	9.76	12.58	37.75
140	36.4	15.11	5.75	-5.79	-5.54	-4.79	-3.97	-4.85	-7.7	-1.34	-7.76	-8.45	-7.69	-5.67	-6.09	-1.9	8.46	11.88	37.82
150	36.28	21.47	0.01	-2.51	-2.21	-2.92	-5.98	-2.92	-8.09	-3.68	-5.7	-5.06	-4.79	-3.88	-6.8	-3.1	8.08	19.34	38.11
160	36.14	19.23	0.3	-0.21	12.65	7.31	-1.41	-1.68	-6.18	1.08	-3.33	-4.45	-4.92	-9.2	-4.72	-3.64	1.35	21.03	37.81
170	36.11	20.82	2.71	0.77	13.04	10.98	8.98	3.14	0.56	7.92	1.87	-3.06	-6.53	-5.2	-2.38	-2.72	3.53	22.53	37.82
180	38.42	34.87	13.27	0.89	6.33	8.66	9.63	7.69	7.08	21.54	9.94	2.55	0.94	-0.4	2.38	4.63	14.14	37.04	40.32

For each engagement simulation, the yaw angle (Y), pitch angle (P), altitude (A), speed of fighter (V), and distance (R) between the weapon system and fighter are varied. The chaff dispensed from the fighter is the ALE-40, provided as a basic model in TESS. The ALE-40 employs three sets of dipoles listed in Table 3 and has a σ_{MaxRCS} of 325.5m², as calculated using Eq. 5. Default values are used for other variables in the weapon system, target, and chaff.

Table 3 Three sets of dipoles resonant at 6, 8, and 10 GHz [18]

Dipole length	Resonant frequency	Number of dipoles
24.1 mm	6.0 GHz	767,000
18.0 mm	8.0 GHz	1,534,000
14.4 mm	10.0 GHz	2,301,000

The engagement simulations varied the values of Y , P , A , V , and R for each scenario, with their minimum, interval, and maximum values shown in Table 4. The simulation was repeated 8,400 times until all variables reached their maximum values with an increasing interval from the minimum values. In addition, the fighter dispensed chaff dispense program calculated using Eqs. (1)-(12) with each variable in each simulation. In some scenarios, the chaff dispense program's BC was calculated as a single burst using the variables because the exposed fighter RCS was lower than one chaff's RCS. In such case, 2 chaffs were applied as the BC , and half of T_c was applied as the BI .

Table 4 The variables in engagement simulation

	Y (Yaw angle)	P (Pitch angle)	A (Altitude)	R (Distance)	V (Speed of fighter)
Min	0°	-30°	1000 m	2000 m	150 m/s
Interval	20°	10°	500 m	1000 m	50 m/s
Max	180°	30°	3000 m	7000 m	300 m/s

As a result of the simulation, it was confirmed that in 41 out of the total 8,400 engagement scenarios, the missile and the fighter had a miss distance within 25m. The miss distance for each engagement scenario is shown in Fig. 3. The x-axis of the graph represents the engagement simulation number, and the y-axis represents the miss distance.

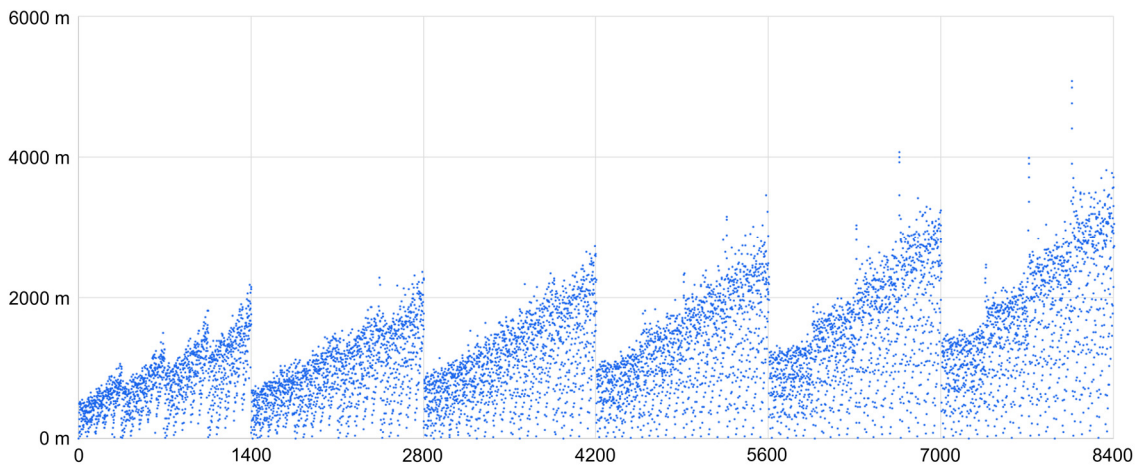


Fig. 3 Miss distance of each scenario

In the 41 cases where the miss distance was within 25m, 39 of them were identified as having a yaw angle (Y) of 0 degrees and a pitch angle (P) lower than 0 degrees. Further analysis of these 39 cases revealed that the missile was moving towards the chaff cloud and the TTR was also tracking the chaff cloud. However, simulations were terminated due to TESS's algorithm determining that the missile could not close in on the target, as the fighter had overlapped with the missile's trajectory. As a result, it can be concluded that the chaff dispense program was successful in deceiving TTR in most engagement scenarios.

4. Conclusions

The study developed a methodology for calculating a chaff dispense program for deceiving TTR by considering various factors such as the fighter, chaff, TTR, and engagement situations. The effectiveness of the chaff dispense program was confirmed through simulations using TESS. The results show that the proposed method can effectively deceive TTRs during engagements. However, the study also identified limitations in the calculation methodology, such as the exclusion of rolling angle from the 3-D angle of aircraft maneuvering for fighter RCS calculation and the lack of consideration for the difference in chaff RCS based on the dispensing order. The calculation results also varied greatly depending on the variables, making it difficult for pilots to calculate and dispense chaff effectively during an engagement. Therefore, further research is needed to optimize the chaff dispense program and address these limitations to improve its effectiveness in various engagement situations and variables.

Acknowledgments

This work was supported by a grant from Hanseo University in 2022.

Conflicts of Interest

The authors declare no conflict of interest.

References

- [1] Y. Li, S. Quan, D. Xiang, W. Wang, C. Hu, Y. Liu, et al., "Ship Recognition from Chaff Clouds with Sophisticated Polarimetric Decomposition," *Remote Sensing*, vol. 12, no. 11, article no. 1813, June 2020.
- [2] B. R. Mahafza, S. C. Winton, and A. Z. Elsherbeni, *Handbook of Radar Signal Analysis (Advances in Applied Mathematics)*, 1st ed., New York: Chapman and Hall/CRC, 2021.
- [3] M. Siddiq, "Deployment of Chaff in Centroid Mode Against Anti-Ship Missiles Using a Variable Azimuth And Elevation Launcher," Ph.D. dissertation, Department System Engineering, Naval Postgraduate School, Monterey, California, September 1989.
- [4] J. Žák, M. Vach, and F. Dvořáček, "Advanced Chaff Usage in Modern EW," *IEEE Radar Methods and Systems Workshop*, pp. 56-59, September 2016.
- [5] X. Wu, Z. Qi, and T. Long, "Research on Applications of Chaff," *8th International Conference on Signal Processing*, vol. 4, November 2006.
- [6] H. U. Shengliang, W. U. Lingang, J. Zhang, and J. Xu, "Research on Chaff Jamming Recognition Technology of Anti-ship Missile Based on Radar Target Characteristics," *12th International Conference on Intelligent Computation Technology and Automation*, pp. 222-226, October 2019.
- [7] D. Y. Lee, J. S. Kim, and D. W. Seo, "Analysis of Effect of Coherent and Incoherent Components on RCS of Chaff Cloud," *Journal of Advanced Marine Engineering and Technology*, vol. 46, no. 3, pp. 128-134, June 2022. (In Korean)
- [8] G. S. Chae, J. S. Lim, and Y. H. Kim, "A RCS Investigation of Multiple Chaff Clouds Using Probability Distribution Characteristics," *Journal of Convergence for Information Technology*, vol. 7, no. 2, pp. 37-42, April 2017. (In Korean)
- [9] L. B. V. Brunt, *Applied ECM: Volume 1*, 1st ed., Madison: EW Engineering, 1978.
- [10] R. E. Fitts, "The Strategy of Electromagnetic Conflict," *Air Force Academy Colo*, February 01, 1979.
- [11] W. Yu, M. Kang, X. Wang, J. Luo, and Y. Sun, "Modeling and Analysis of Fire Control Radar Capabilities Against Passive Jamming," *Man-Machine-Environment System Engineering: Proceedings of the 19th International Conference on MMESE*, pp. 485-491, August 2019.
- [12] *Handbook for Chaff*, Leonardo, 2022.
- [13] *Handbook for Employment of Chaff*, Tracor.
- [14] D. C. Shin, C. H. Lee, D. H. Kim, Y. L. Rhie, and Y. H. Choi, "A Study on the Integration Method of Threat Environment Engineering Models in Electronic Warfare SILS System," *Proceedings of Symposium of the Korean Institute of Communications and Information Sciences*, pp. 295-296, February 2020. (In Korean)
- [15] C. H. Park, "Development of an Electromagnetic Wave Service and Modeling of an Electromagnetic Wave Transmitting/Receiving Environment for Open Architecture Radar Electronic Warfare Simulations," M.S. dissertation, Department Aerospace Engineering, Sejong University, Seoul, February 2019. (In Korean)
- [16] J. I. Jo, J. H. Lee, and J. M. Ahn, "A Study on the Jamming Technique for Monopulse Missile Using TESS(Tactical Engagement Simulation Software)," *Proceedings of Symposium of the Korean Institute of Communications and Information Sciences*, pp. 707-708, June 2017. (In Korean)
- [17] O. Widlund, S. Nais, and J. Hawkes, *Janes Land Warfare Platform-Artillery & Air Defence 2022-2023*, Coulsdon, Jane's Information Group, 2022.
- [18] B. C. F. Butters, "Chaff," *IEE Proceedings F: Communications Radar and Signal Processing*, vol. 129, no. 3, pp. 197-201, June 1982.



Copyright© by the authors. Licensee TAETI, Taiwan. This article is an open access article distributed under the terms and conditions of the Creative Commons Attribution (CCBY) license (<http://creativecommons.org/licenses/by/4.0/>).